

# Correlation between electrical properties and crystalline phases for ZnO-Bi<sub>2</sub>O<sub>3</sub> based varistor ceramics with rare earth additives

Tomoaki Kato · Yoshio Takada

Received: 16 September 2012 / Accepted: 1 April 2013 / Published online: 13 April 2013  
© The Author(s) 2013. This article is published with open access at Springerlink.com

**Abstract** In this study, the correlation between the electrical properties and crystalline phases of ZnO-Bi<sub>2</sub>O<sub>3</sub> based varistor ceramics with rare earth additives was investigated. The additives used were in the form R<sub>2</sub>O<sub>3</sub>, where R represents Eu, Ho, Y, Er, Yb, or Lu. It was found that the incorporation of rare earth additives led to an increase in the varistor voltage in the nonlinear region, an increase in the leakage current in the pre-breakdown region, and a reduction in the limiting voltage in the upturn region. In the sample with added Y<sub>2</sub>O<sub>3</sub>, a phase referred to as the R-phase, which contained Y, Bi, Sb, Zn, Mn, and O, was observed to be homogeneously distributed at ZnO grain boundaries. X-ray diffraction analysis revealed that the amount of the Zn-Sb-O spinel and Bi-Cr-O phases present was reduced by the rare earth addition, and that rare earth elements were incorporated into a common crystalline phase. It is suggested that the formation of the R-phase at ZnO grain boundaries and the reduction in the Bi<sub>2</sub>O<sub>3</sub> liquid phase during the sintering process might be responsible for suppressing ZnO grain growth, thus leading to an increase in the varistor voltage.

**Keywords** Ceramics · Varistor · ZnO · Microstructure · Electrical properties

---

T. Kato (✉)  
Advanced Technology R&D Center, Mitsubishi Electric Corporation, Amagasaki, Hyogo 661-8661, Japan  
e-mail: Kato.Tomoaki@dy.mitsubishielectric.co.jp

Y. Takada  
Transmission and Distribution Systems Center, Mitsubishi Electric Corporation, Amagasaki, Hyogo 661-8661, Japan

## 1 Introduction

ZnO varistor ceramics exhibit unique voltage-current behavior and are widely used for protecting electrical and electronic devices from lightning and other power surges [1]. It is well known that this unique behavior is derived from the nonlinear voltage-current (V-I) characteristics of ZnO-ZnO grain boundaries. ZnO is an n-type semiconductor, and its electrical resistivity can be easily controlled with doping with trivalent elements such as Al and Ga [2, 3]. Bi<sub>2</sub>O<sub>3</sub> is typically used as an additive to confer nonlinear V-I characteristics at the ZnO-ZnO grain boundaries. This is brought about by the formation of double Schottky barriers at the grain boundaries, whose breakdown voltage is roughly 3 V. To further enhance the nonlinear V-I characteristics, small amounts of transition elements such as Co, Mn, Cr, and Ni are commonly added to varistor ceramics, while Sb and Si are added to increase the varistor voltage [4]. R. Einzinger reported that an additional SiO<sub>2</sub> dissolves in Bi<sub>2</sub>O<sub>3</sub> and increase the viscosity of the liquid [5].

Since the varistor voltage per unit area of grain boundary is fairly constant, in order to increase the overall varistor voltage without changing the varistor thickness, it is necessary to increase the number of grain boundaries, i.e., decrease the ZnO grain size. This can be achieved by the addition of Sb or Si. It has also been shown that the addition of R<sub>2</sub>O<sub>3</sub> (R: rare earth element) leads to a reduction in the ZnO grain size and an increase in the varistor voltage [6–16]. It was reported that a new phase containing the rare earth element (referred to as the R-phase) segregates at ZnO grain boundaries. This phase consists of R-Bi-Sb-Zn-(Mn)-O [6] and is strongly involved in the suppression of ZnO grain growth during the sintering process

[7–10]. It was found that the addition of  $R_2O_3$  gave rise to a significant increase in the varistor voltage and leakage current, in addition to a larger energy absorption capacity.

Capacitance-voltage (C-V) measurements [17] revealed that  $R_2O_3$  addition to ZnO-Bi<sub>2</sub>O<sub>3</sub> based varistor ceramics had a significant effect on the double Schottky barrier (DSB) parameters, in that the donor density ( $N_D$ ) and the density of interface states ( $N_S$ ) were increased, while the barrier height ( $\Phi_B$ ) was decreased. Bernik et al. concluded that the larger rise in  $N_D$  was the main factor contributing to the decrease in  $\Phi_B$  [7], and thus the increase in the leakage current. Several authors have also reported the electrical degradation of ZnO varistor ceramics with  $Y_2O_3$  and  $ZrO_2$  additives, and the effect of  $R_2O_3$  additives on the performance of lightning arresters based on ZnO varistor ceramics [18].

Since a high varistor voltage can allow downsizing of surge arresters, ZnO-Bi<sub>2</sub>O<sub>3</sub> based varistor ceramics with  $R_2O_3$  additives have been an active field of research. Previous studies have shown that the sintering temperature used to produce varistor ceramics often has an important influence not only on electrical properties such as the varistor voltage, nonlinear coefficient ( $\alpha$ ), and leakage current, but also on the presence of crystalline phases such as the ZnO phase, the Zn-Sb-O spinel phase, the Bi-rich phase, and the R-phase in the sintered body [12, 15]. Nevertheless, although there has been a large amount of research on the effect of  $R_2O_3$  addition on the electrical properties, few studies have compared the electrical properties and the crystalline phases under identical processing conditions.

The objective of the present research is to investigate the correlation between the electrical properties and crystalline phases of ZnO-Bi<sub>2</sub>O<sub>3</sub> based varistor ceramics with  $R_2O_3$  additives under identical processing conditions. The additives used were  $Eu_2O_3$ ,  $Ho_2O_3$ ,  $Y_2O_3$ ,  $Er_2O_3$ ,  $Yb_2O_3$ , and  $Lu_2O_3$ , which are known to significantly enhance the varistor voltage. The ionic radii of  $Eu^{3+}$ ,  $Ho^{3+}$ ,  $Y^{3+}$ ,  $Er^{3+}$ ,  $Yb^{3+}$ , and  $Lu^{3+}$  have been

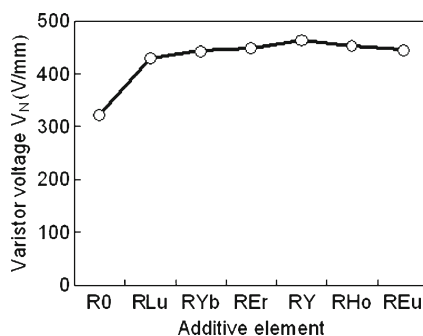


**Fig. 1** Dependence of varistor voltage ( $V_N$ ) on type of rare earth additive. R0, rare earth free; RLu, R0+Lu<sub>2</sub>O<sub>3</sub>; RYb, R0+Yb<sub>2</sub>O<sub>3</sub>; REr, R0+Er<sub>2</sub>O<sub>3</sub>; RY, R0+Y<sub>2</sub>O<sub>3</sub>; RHo, R0+Ho<sub>2</sub>O<sub>3</sub>; REu, R0+Eu<sub>2</sub>O<sub>3</sub>

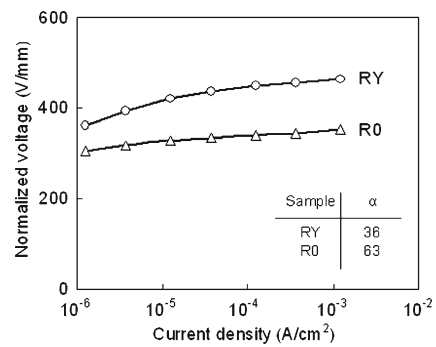


**Fig. 2** E-J characteristic of sample RY (contained 0.5 mol%  $Y_2O_3$ ) and sample R0 (rare earth free)

reported to be 0.0947, 0.0901, 0.09, 0.089, 0.0868, and 0.0861 nm, respectively [19]. Thus, in terms of increasing ionic radius, the sequence is  $Lu^{3+} < Yb^{3+} < Er^{3+} < Y^{3+} < Ho^{3+} < Eu^{3+}$ .

## 2 Experimental

Samples were prepared by a conventional ceramic fabrication process from industrial grade powders. A reference sample (labeled R0) was produced using ZnO containing 0.5 mol% Bi<sub>2</sub>O<sub>3</sub>, 1.2 mol% Sb<sub>2</sub>O<sub>3</sub>, and small amounts of other elements such as Co, Mn, Ni, Cr, Si, Al, and B. Reagent grade rare earth oxides were used as additives to this basic composition. The additives used were  $Y_2O_3$ ,  $Eu_2O_3$ ,  $Ho_2O_3$ ,  $Er_2O_3$ ,  $Yb_2O_3$ , and  $Lu_2O_3$ , and the resulting samples are referred to as RY, REu, RHo, REr, RYb, and RLu, respectively. The amount of rare earth oxide was fixed at 0.5 mol%. The mixed powders, with the exception of ZnO, were ball milled for 16 h in distilled water. The resulting slurry, ZnO, and polyvinyl alcohol as a binder were then mixed using a blender. The granulated powder was pressed at 39 MPa into pellets 40 mm in diameter and 10 mm thick. The pressed pellets were sintered at 1,150 °C for 5 h in an O<sub>2</sub> atmosphere with heating and cooling rates of 75 °C/h. The diameter of sintered samples were 32 mm,

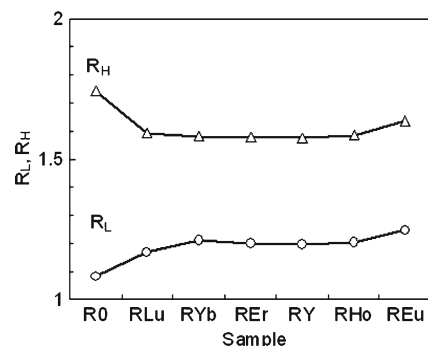
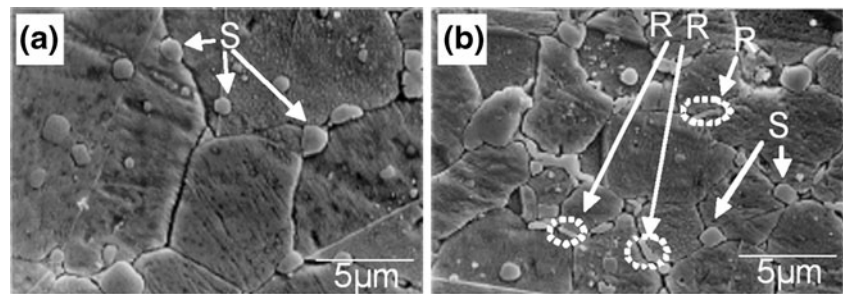


**Fig. 3** Correlation between  $R_L$ ,  $R_H$  and the rare earth additive.  $R_L$ ,  $V_{1mA}/V_{10\mu A}$ ;  $R_H$ ,  $V_{2.5kA}/V_{1mA}$

**Fig. 4** Surface microstructure of ZnO-Bi<sub>2</sub>O<sub>3</sub> based varistor ceramics: **a** R0 (rare earth free), **b** RY (R0+0.5 mol% Y<sub>2</sub>O<sub>3</sub>). R R-phase, S Zn-Sb-O spinel



and the shrinkage after sintering was approximately 20 %. Aluminum electrodes were spray coated onto the surface of the sintered body to evaluate the electrical properties.

The electrical properties of each sample were evaluated using a high-voltage DC source. Microstructural observations and analysis were carried out using an electron probe microanalysis (EPMA) system (JXA-8621MX, JEOL, Japan). The surface of the samples used for EPMA analysis was polished with a diamond paste (1 μm) and chemically etched with a 10 %-NaOH aqueous solution for a few minutes. The average ZnO grain size ( $D$ ) in each sample was determined by the line-intercept method [20]. The crystalline phases present in the samples were analyzed using powder X-ray diffraction (XRD) with CuK $\alpha$  radiation (MXP18V, Bruker AXS). The X-ray tube voltage and current were fixed at 40 kV and 200 mA, respectively.

### 3 Results and discussion

The dependence of the varistor voltage  $V_N$  (V/mm) on the type of rare earth additive are shown in Fig. 1. Here,  $V_N$  is defined as the voltage required to produce a current of 1 mA. As seen in the figure, samples with a rare earth additive exhibit a significantly higher varistor voltages

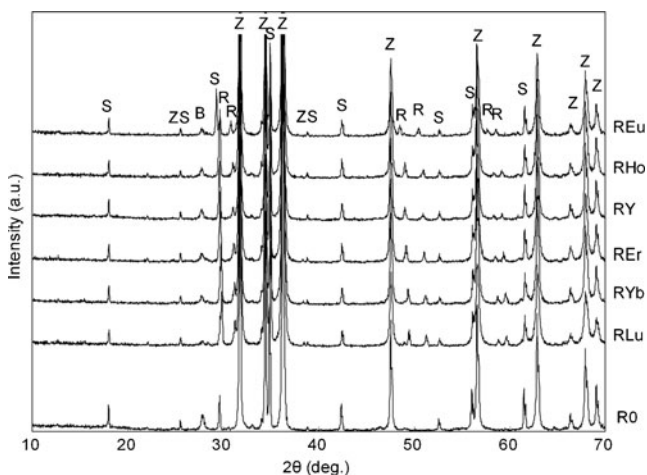


**Fig. 5** XRD patterns from ZnO varistor ceramics. Z ZnO (36-1451), S Zn-Sb-O spinel phase (15-0517), ZS Zn<sub>2</sub>SiO<sub>4</sub> phase (37-1485), B Bi-Cr-O phase (37-0958), R R-phase. () shows the JCPDF No

(430–463 V/mm) compared to sample R0 (323 V/mm). The E-J characteristic of sample RY (contained 0.5 mol% Y<sub>2</sub>O<sub>3</sub>) and R0 is shown in Fig. 2. In the pre-breakdown region, a leakage current property in the E-J curve and the lower value of  $\alpha$ , which is calculated by the current flow of 0.1 mA and 1 mA were observed in sample RY.

The electrical properties in the pre-breakdown and upturn regions were also examined [21], and the results are shown in Fig. 3. In the pre-breakdown and upturn regions, the electrical properties are characterized by the parameters  $R_L$  ( $=V_{1mA}/V_{10\mu A}$ ) and  $R_H$  ( $=V_{2.5kA}/V_{1mA}$ ), respectively. Here,  $V_{1mA}$ , for example, represents the voltage required to produce a current of 1 mA. An impulse voltage was used to determine the value  $V_{2.5kA}$ . As seen in Fig. 3, all samples with rare earth additives exhibit larger  $R_L$  values than sample R0. This can be thought of in terms of an increase in the leakage current. In can also be seen that the rare earth additives cause a decrease in  $R_H$ . As several authors have already pointed out, the effect of R<sub>2</sub>O<sub>3</sub> additives on the electrical characteristics is related to variations in DSB parameters such as  $N_D$ ,  $N_S$ , and  $\Phi_B$  [7, 14]. It has been suggested that the increase in  $R_L$  in the pre-breakdown region is mainly due to a decrease in  $\Phi_B$ , whereas in the upturn region, the decrease in  $R_H$  is mainly the result of an increase in  $N_D$ , i.e., a decrease in the resistance of ZnO grains [7].

It has been reported that for a Y<sub>2</sub>O<sub>3</sub> additive, trivalent Y<sup>3+</sup> cations may replace divalent Zn<sup>2+</sup> cations in the ZnO lattice, thus leading to an increase in  $N_D$  [10, 14]. As seen in Fig. 3, except for samples RLu and REu, the  $R_L$  and  $R_H$  values are similar for all samples with R<sub>2</sub>O<sub>3</sub> additives.

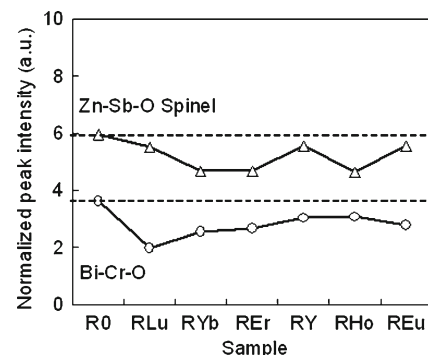


**Fig. 6** XRD peak intensity of Zn-Sb-O spinel phase and Bi-Cr-O phase for different rare earth additives

Since, of the six rare earth elements used in this study, Lu has the smallest ionic radius Eu has the largest, the effect of Lu or Eu addition on  $R_L$  and  $R_H$  may involve dissolved  $R^{3+}$  cations in the ZnO grains.

Figure 4 shows scanning electron microscopy (SEM) images of the surface microstructure in samples R0 and RY. The ZnO grain size in sample RY ( $D=6.5 \mu\text{m}$ ) was found to be significantly smaller than that in sample R0 ( $D=10.3 \mu\text{m}$ ). In sample RY, Zn-Sb-O spinel particles,  $\text{Zn}_2\text{SiO}_4$ , and columnar particles (R-phase) were homogeneously distributed at ZnO grain boundaries. In addition, some small Zn-Sb-O spinel particles were observed within ZnO grains. As shown in Fig. 4, the R-phase particles were relatively small ( $< 1 \mu\text{m}$ ) and were surrounded by other phases such as ZnO and Zn-Sb-O. Kato et al. revealed that the R-phase consisted of Y, Bi, Sb, Zn, and O, and the atomic ratio was Y: Bi: Sb: Zn=35: 8: 35: 22. (atom. %) As is pointed out by some authors [6–8, 10, 11, 15, 16], the presence of the segregated R-phase at ZnO grain boundaries may be responsible for the increase in varistor voltage due to suppression of ZnO grain growth during the sintering process.

Figure 5 shows XRD diffraction patterns from the samples used in the present study. The diffraction peaks were classified as ZnO, Bi-Cr-O ( $\text{Bi}_{16}\text{CrO}_{27}$ ), Zn-Sb-O spinel,  $\text{Zn}_2\text{SiO}_4$ , and the R-phase. The peaks labeled R could be identified as being associated with the R-phase since these peaks were not observed for sample R0, and SEM observations identified no additional crystalline phases in the samples with rare earth additives. Moreover, it can clearly be seen in Fig. 5 that the peaks associated with the R-phase undergo a shift towards lower angles, depending on the type of additive. It is possible that the magnitude of this shift may be related to the ionic radius of the rare earth element. Thus, in terms of increasing ionic radius, the sequence is  $\text{Lu}^{3+} < \text{Yb}^{3+} < \text{Er}^{3+} < \text{Y}^{3+} < \text{Ho}^{3+} < \text{Eu}^{3+}$ , which also corresponds to that for the magnitude of the peak shift in Fig. 5. Thus, the lattice spacing of the R-phase increases with the ionic radius of the rare earth element. This result also suggests that the rare earth elements are incorporated into a common crystalline phase at the ZnO grain boundaries, which can be assumed to behave similarly in ZnO- $\text{Bi}_2\text{O}_3$ -based varistor ceramics.

Based on the results shown in Fig. 5, the reason for the increase in the varistor voltage due to the rare earth additives can now be discussed.

Figure 6 shows the relative amount of the Zn-Sb-O spinel phase (labeled S in Fig. 5) and the Bi-Cr-O phase (labeled B in Fig. 5) in each sample, based on the XRD peak intensity. Each peak was normalized relative to the ZnO(101) peak ( $2\theta=36.26^\circ$ ). With addition of  $\text{R}_2\text{O}_3$ , the relative amount of both the Zn-Sb-O spinel and Bi-Cr-O phases decreased. This may be due to consumption of Bi and Sb to form the R-phase during the sintering process. It is well known that the formation of a  $\text{Bi}_2\text{O}_3$  liquid phase during sintering

accelerates ZnO grain growth, resulting in a low varistor voltage. In addition, the formation of the Zn-Sb-O spinel phase during sintering is expected to decelerate ZnO grain growth, resulting in a high varistor voltage. Also, it has been reported by several authors that the formation of the R-phase at ZnO grain boundaries may cause grain boundary pinning that suppresses ZnO grain growth, resulting in a high varistor voltage [6, 10]. Thus, it can be assumed that the increase in varistor voltage due to the rare earth additive is mainly the result of R-phase formation and the associated reduction in the amount of the  $\text{Bi}_2\text{O}_3$  liquid phase that is formed. Since Fig. 1 shows that the varistor voltage exhibits very little dependence on the type of rare earth additive used, it is likely that it is the fact that the R-phase is formed, rather than what its composition is, that is most responsible for increasing the varistor voltage.

However, Xu et al. recently reported that doping with rare earth oxides affects the formation and decomposition of  $\text{Bi}_3\text{Zn}_2\text{Sb}_3\text{O}_{14}$  pyrochlore [15]. Continuous seeking for a formation mechanism of R-phase, pyrochlore, and Zn-Sb-O spinel during the sintering with  $\text{R}_2\text{O}_3$  additive should be required.

## 4 Conclusions

A comparative study has been carried out on the effect of  $\text{R}_2\text{O}_3$  ( $\text{R}=\text{Eu, Ho, Y, Er, Yb, Lu}$ ) additives on the electrical properties and crystalline phases of ZnO- $\text{Bi}_2\text{O}_3$  based varistor ceramics. The  $\text{R}_2\text{O}_3$  additives caused a significant increase in the varistor voltage and the parameter  $R_L$  in the pre-breakdown region, and a decrease in the parameter  $R_H$  in the upturn region. An R-phase with a composition of R-Bi-Sb-Zn-O was found to be homogeneously segregated at ZnO grain boundaries in samples with rare earth additives. XRD analysis revealed that the rare earth elements are incorporated into this phase, which has a common crystal structure but varying lattice constants. Formation of the R-phase, a decrease in Zn-Sb-O spinel phase, a decrease in the  $\text{Bi}_2\text{O}_3$  liquid phase, and an increase in the varistor voltage occurred simultaneously by the addition of rare earth elements. The R-phase is thought to play a dominant role in enhancing the varistor voltage.

**Open Access** This article is distributed under the terms of the Creative Commons Attribution License which permits any use, distribution, and reproduction in any medium, provided the original author(s) and the source are credited.

## References

1. M. Matsuoka, Jpn. J. Appl. Phys. **10**, 736 (1971)
2. W.G. Carlson, T.K. Gupta, J. Appl. Phys. **53**, 5746 (1982)
3. T.K. Gupta, J. Mater. Res. **9**, 2213 (1994)
4. T.R.N. Kutty, S. Ezhilvalavan, J. Phys. D: Appl. Phys. **29**, 809 (1996)
5. R. Einzinger, Annu. Rev. Mater. Sci. **17**, 299 (1987)

6. T. Kato, A. Hori, S. Yamashita, Y. Takada, *TIEEJ* **120-B**, 968 (2000)
7. S. Bernik, S. Macek, B. Ai, J. *Eur. Ceram. Soc.* **21**, 1875 (2001)
8. S. Bernik, S. Macek, B. Ai, J. *Eur. Ceram. Soc.* **24**, 1195 (2004)
9. M. Houabes, R. Metz, *Ceram. Int.* **33**, 1191 (2007)
10. J. Yoon, C. Lee, K. Lee, H. Lee, S. Lee, *Trans. Electr. Electron. Mater.* **10**, 152 (2009)
11. M.A. Ashraf, A.H. Bhuiyan, M.A. Hakim, M.T. Hossain, *Physica B* **405**, 3770 (2010)
12. D. Xu, X. Shi, X. Cheng, J. Yang, Y. Fan, H. Yuan, L. Shi, *Trans. Nonferrous Met. Soc. China* **20**, 2303 (2010)
13. M.A. Ashraf, A.H. Bhuiyan, M.A. Hakim, M.T. Hossain, *Mater. Sci. Eng.B* **176**, 855 (2011)
14. J. He, J. Liu, J. Hu, W. Long, *Mater. Lett.* **65**, 2595 (2011)
15. D. Xu, D. Tang, Y. Lin, L. Jiao, G. Zhao, X. Cheng, *J. Cent. South Univ. Technol.* **19**, 1497 (2012)
16. Y. Akiyama, A. Fukumori, M. Takada, Y. Sato, S. Yoshikado, *IEEJ Trans. FM.* **130**, 394 (2010)
17. K. Mukae, K. Tsuda, I. Nagasawa, *J. Appl. Phys.* **50**, 4475 (1979)
18. S. Shichimiya, M. Yamaguchi, N. Furuse, M. Kobayashi, S. Ishibe, *IEEE Trans. Power Delivery* **13**, 465 (1998)
19. R.D. Shannon, *Acta Cryst.* **A32**, 751 (1976)
20. M.I. Mendelson, *J. Am. Ceram. Soc.* **52**, 443 (1969)
21. T.K. Gupta, *J. Am. Ceram. Soc.* **73**, 1817 (1990)